Neurotox Res (2015) 28:290–301
DOI 10.1007/s12640-015-9539-7

ORIGINAL ARTICLE

NMR-Based Metabolic Profiling Reveals Neurochemical Alterations in the Brain of Rats Treated with Sorafenib

Changman Du[1] · Xue Shao[1] · Ruiming Zhu[1] · Yan Li[1] · Qian Zhao[1] · Dengqi Fu[1] · Hui Gu[1] · Jueying Kong[1] · Li Luo[1] · Hailei Long[1] · Pengchi Deng[3] · Huijuan Wang[2] · Chunyan Hu[1] · Yinglan Zhao[2] · Xiaobo Cen[1]

Received: 9 April 2015 / Revised: 22 June 2015 / Accepted: 1 July 2015 / Published online: 2 August 2015

Abstract Sorafenib, an active multi-kinase inhibitor, has been widely used as a chemotherapy drug to treat advanced clear-cell renal cell carcinoma patients. In spite of the relative safety, sorafenib has been shown to exert a negative impact on cognitive functioning in cancer patients, specifically on learning and memory; however, the underlying mechanism remains unclear. In this study, an NMR-based metabolomics approach was applied to investigate the neurochemical effects of sorafenib in rats. Male rats were once daily administrated with 120 mg/kg sorafenib by gavage for 3, 7, and 28 days, respectively. NMR-based metabolomics coupled with histopathology examinations for hippocampus, prefrontal cortex (PFC), and striatum were performed. The ^{1}H NMR spectra data were analyzed by using multivariate pattern recognition techniques to show the time-dependent biochemical variations induced by sorafenib. Excellent separation was obtained and distinguishing metabolites were observed between sorafenib-treated and control rats. A total of 36 differential metabolites in hippocampus of rats treated with sorafenib were identified, some of which were significantly changed. Furthermore, these modified metabolites mainly reflected the disturbances in neurotransmitters, energy metabolism, membrane, and amino acids. However, only a few metabolites in PFC and striatum were altered by sorafenib. Additionally, no apparent histological changes in these three brain regions were observed in sorafenib-treated rats. Together, our findings demonstrate the disturbed metabonomics pathways, especially, in hippocampus, which may underlie the sorafenib-induced cognitive deficits in patients. This work also shows the advantage of NMR-based metabolomics over traditional approach on the study of biochemical effects of drugs.

Keywords Metabolomic · NMR · Sorafenib · Neurotoxicity

Introduction

Chemotherapeutic drugs are known to cause significant clinical neurotoxicity, which results in early cessation of treatment (Kuroi and Shimozuma 2004). Cognitive impairment is reported by as many as 70 % of patients who experienced cancer therapy (Dietrich et al. 2008); moreover, up to 50 % of patients report significant and measurable declines in attention, learning, memory, and overall processing speed (Vardy and Tannock 2007). Candidate mechanisms have been suggested to contribute to the neurotoxicity, such as direct neurotoxic effects of chemotherapy, oxidative damage, immune dysregulation, and genetic predisposition (Ahles and Saykin 2007).

Sorafenib, an orally active multi-kinase inhibitor that can cross the blood–brain barrier, has been widely used as a

Electronic supplementary material The online version of this article (doi:10.1007/s12640-015-9539-7) contains supplementary material, which is available to authorized users.

✉ Xiaobo Cen
xbcenalan@sina.com; xbcen@scu.edu.cn

[1] National Chengdu Center for Safety Evaluation of Drugs, State Key Laboratory of Biotherapy and Cancer Center, West China Hospital, Sichuan University, and Collaborative Innovation Center for Biotherapy, #1 Keyuan Road 4, Gaopeng Street, High-tech Development Zone, Chengdu 610041, China

[2] State Key Laboratory of Biotherapy and Cancer Center, West China Hospital, Sichuan University, and Collaborative Innovation Center for Biotherapy, Chengdu 610041, China

[3] Analytical and Testing Center, Sichuan University, Chengdu, Sichuan, China

chemotherapy drug to treat advanced clear-cell renal cell carcinoma patients (Takimoto and Awada 2008). It selectively targets vascular endothelial growth factor receptor (VEGFR) 2/3, Raf, platelet-derived growth factor receptor, FLT-3, as well as c-Kit (Kane et al. 2006). In recent years, sorafenib, however, has been shown to exert a negative impact on cognitive functioning in cancer patients, specifically on learning and memory, and executive functioning (Mulder et al. 2014; Brandi et al. 2013). Patient groups performed significantly worse on the cognitive functions compared to healthy controls. Effect sizes of cognitive dysfunction in patients using sorafenib were larger than patient controls (Mulder et al. 2014). Although VEGF has been implicated to affect cognitive functioning through its effects on neurogenesis, cerebral blood flow, and/or modulation of long-term potentiation (Schänzer et al. 2004; Ongali et al. 2010; Fournier et al. 2013), the neurochemical mechanism underlying such effects remains unknown (Kane et al. 2006; Mulder et al. 2014).

Currently, metabonomics has been widely applied in neurotoxicity and neuropsychiatric research fields, such as motor neuron disease, Parkinson's disease, and drug neurotoxicity (Kaddurah-Daouk and Krishnan 2009; McClay et al. 2013). Metabolomics acts as a powerful tool for detecting variations in a range of intracellular metabolites upon drug exposure (Duarte et al. 2013). Unlike genomics, transcriptomics, or proteomics, metabonomics shows what indeed happens and detects the metabolite profile, thus, having a potential to identify the related molecules or biomarkers involved in neuropathological process. Nuclear magnetic resonance (NMR) is one of the commonly applied analytical techniques to assay and quantify metabolites (Kaddurah-Daouk et al. 2008). It is be able to uncover the intricate relationship between drug-induced neurological changes and crucial endogenous metabolites, providing new insights into the pathological processes and mechanisms of neurotoxicity (Li et al. 2014; Krishnan et al. 2005; Jung et al. 2011).

In this work, NMR-based metabolomics methods coupling with histopathology methods were used to investigate the neuropathological effects of sorafenib. We found that sorafenib leads to disturbances in neurotransmitters, energy metabolism, membrane metabolism, as well as antioxidant in the hippocampus of rats. Our findings provide an in-depth insight into the neurochemical abnormality associated with sorafenib-related cognitive impairments in patients.

Materials and Methods

Drugs

Studies employed commercially available chemicals as follows: deuterium oxide (99.8 %) (NORELL, Landisville, USA), trimethylsilylpropionic acid-d4 sodium salt (TSP) (Sigma Aldrich, St. Louis, MO), HPLC-grade methanol, and chloroform (Fisher Scientific, Fairlawn, NJ, USA). Sorafenib (Nanjing PharmaBlock, China) was diluted with 5 % sodium carboxymethyl solution (CMC-Na) prior to use.

Animals

Male Sprague–Dawley rats, weighing 200–220 g, were purchased from Beijing Vital River Laboratories Company (China). All animals were housed five per cage under controlled conditions of light (12/12-h light–dark cycle) with free access to food and water. After 7 days of acclimatization, rats were used for experiments. All animal experiments in this study were carried out in accordance with the guidelines established by the Association for Assessment and Accreditation of Laboratory Animal Care (AAALAC).

Animal Treatments

Animals were weighted and randomly divided into control and sorafenib groups with 24 rats per group. The rats in control group received 5 % CMC-Na, while the rats in sorafenib group were administrated with sorafenib (120 mg/kg body weight) by gavage for 3, 7, and 28 days, respectively.

Preparation and Extraction of Brain Samples

At the end of each administration period, rats were sacrificed by rapid decapitation. The left brain of hippocampus, striatum, and prefrontal cortex (PFC) were rapidly dissected, snap-frozen in liquid nitrogen, and stored at −80 °C until analysis (Salek et al. 2008; Wang et al. 2013a). The right brains were rapidly fixed in 10 % formalin.

The frozen tissue samples were suspended in methanol (4 ml per gram of tissue) and double distilled water (0.85 ml/g of tissue). After vortex, chloroform (2 ml/g of tissue) was added, followed by additional 50 % chloroform (2 ml/g of tissue). The suspension was kept on ice for 30 min, and then centrifuged at $1000\times g$ for 30 min at 4 °C. This procedure separated suspension into three phases: a water phase at the top, a denatured proteins phase in the middle, and a lipid phase at the bottom. The upper phase (aqueous phase) of each sample was collected and evaporated to dryness under a stream of nitrogen. The residue was reconstituted with 580 µl of D_2O containing 0.01 mg/ml sodium (3-trimethylsilyl)-2,2,3,3-tetradeuteriopropionate (TSP). The D_2O and TSP provided the deuterium lock signal for the NMR spectrometer and the chemical shift reference (δ 0.0), respectively. After being centrifuged at $12{,}000\times g$ for 5 min, the supernatant was

transferred into a 5-mm NMR tube for NMR spectroscopy (Beckonert et al. 2007).

^{1}H NMR Spectroscopic Analysis

All tissue samples were analyzed by ^{1}H NMR spectroscopy at 600.13 MHz using a Bruker Avance II 600 spectrometer operating (Bruker Biospin, Germany) at 300 K. A one-dimensional spectrum was acquired by using a standard (1D) Carr–Purcell–Meiboom–Gill pulse sequence to suppress the water signal with a relaxation delay of 5 s. Sixty-four free induction decays (FIDs) were recorded by 64 K data points with a spectral width of 12,335.5-Hz spectral, an acquisition time of 2.66 s, and a total pulse recycle delay of 7.66 s. The FIDs were weighted by a Gaussian function with line-broadening factor −0.3 Hz, Gaussian maximum position 0.1, prior to Fourier transformation (Hu et al. 2012).

Pattern Recognition (PR) Analysis

The ^{1}H NMR spectra were processed using MestReNova-6.1.1-6384 software before data processing. All the spectra were corrected for phase and baseline distortions using MestReNova-6.1.1-6384 software. The ^{1}H NMR spectra of tissue samples were referenced to the TSP resonance at δ 0.0. The spectrum ranging from 9.8 to 0.5 ppm was divided into 2325 integral segments of equal length (0.004 ppm). The area under the spectrum was calculated for each segmented region and expressed as an integral value. The region 5.1–4.6 ppm was removed for excluding the effect of imperfect water signal. Moreover, the integrated data were normalized before multivariate statistical analysis to eliminate the dilution or bulk mass differences among samples due to the different weight of tissue, and to give the same total integration value for each spectrum.

Multivariate statistical analysis was performed to process the acquired NMR data using SIMCA-P+11 (Umetrics, AB). The principal component analysis (PCA) was initially applied to analyze the NMR spectral data to separate drug samples from normal samples. The data were visualized using the principal component (PC) score plots to identify general trends and outliers. Orthogonal projection to latent structure with discriminant analysis (OPLS-DA) was subsequently used to improve the separation. The default seven-round cross-validation was applied with one-seventh of the samples being excluded from the mathematical model in each round, in order to guard against over fitting. The model coefficients locate the NMR variables associated with specific interventions as y variables. The model coefficients were then back-calculated from the coefficients incorporating the weight of the variables in order to enhance interpretability of the model: in the coefficient plot, the intensity corresponds to the mean-centered model (variance) and the color scale derives from the unit variance-scaled model (correlation). The coefficient plots were generated with Matlab scripts with some in house modifications and were color-coded with the absolute value of coefficients.

To identify the variables contributed to the assignment of spectra between experimental group and normal controls, the variable importance in the projection (VIP) values of all peaks from OPLS-DA models was analyzed, and variables with VIP > 1 were considered relevant for group discrimination. Moreover, unpaired Student's t test ($p < 0.05$) to the chemical shifts was also used to assess the significance of each metabolite. Only both VIP > 1 of multivariate and $p < 0.05$ of univariate statistical significance were identified as distinguishing metabolites. The corresponding chemical shift and multiplicity of the metabolites were identified by comparisons with the previous literature and the Human Metabolome Database (http://www.hmdb.ca/), a web based bioinformatics/cheminformatics resource with detailed information about metabolites and metabolic enzymes (Wang et al. 2013b).

Histopathological Examination

Histopathological assessments were performed with the standard procedures. In brief, the formalin-fixed hippocampus, striatum, and cortex tissues were embedded in paraffin wax, sectioned (3–4 μm), and stained with the hematoxylin and eosin, followed by microscopic assessments.

Results

General Symptoms of Rats

No significant changes were found in the body weight of rats treated with sorafenib for 3, 7, or 28 days continuously in comparison to the control rats (Supplementary Fig. 1). Furthermore, the rats treated with sorafenib also showed no abnormal neurobehavior during drug administration.

Histopathology

HE staining revealed no remarkable neuronal abnormalities in the hippocampus, striatum, and PFC of rats from both control and sorafenib-treated rats. The pyramidal cells in the hippocampus region were arranged neatly and tightly, and no cell loss was found in brain of sorafenib-treated rats. Hippocampal cells were round and intact with nuclei stained clear (Fig. 1). Other two brain regions also showed no abnormality (Supplementary Fig. 2).

^{1}H NMR Spectra

Representative ^{1}H NMR spectra of the three cerebral regions after sorafenib or vehicle administration are shown in Fig. 2. The standard one-dimension spectrum gave an overview of all metabolites. The major metabolites in the integrate regions were identified by a comparison with literature data (Gao et al. 2007; Xiang et al. 2006) and spectra of standards acquired in Human Metabolome Database (http://www.hmdb.ca/) (Wishart et al. 2007). As a result, a series of changes in endogenous metabolite levels were observed in sorafenib-treated rats when compared with the brain tissue from control rats. These metabolites included γ-aminobutyric acid (GABA), glutamate, glutamine, α-glucose, lactate, acetoacetate, α-ketoglutarate, trimethylamine-N-oxide (TMAO), creatine, phosphocreatine, choline, phosphocholine, myo-inositol, and taurine. Of these modified metabolites, neurotransmitters, energy metabolism, and membrane components were markedly altered.

PR Analysis of Metabolites

To determine the differences between the vehicle-treated and sorafenib-administrated rats, we initially utilized the PCA to analyze ^{1}H NMR data after data normalization. The results showed an apparent separation between sorafenib-treated brain tissues and normal controls on the scores plot of first two principal components PC (Fig. 3). The majority of samples were located in 95 % confidence interval. Therefore, all samples were used in the following analysis to ensure the maximum information.

To identify the main metabolites responsible for the separation between the control and sorafenib groups, their scores and loadings plots with correlation coefficients were obtained from OPLS-DA analysis based on NMR data. The scores plots of PC1 and PC2 showed that the hippocampus of sorafenib-treated rats was clearly distinguished from normal controls (Fig. 3). The scores plots of PC1 and PC2 for striatum and PFC are shown in Supplementary Figs. 3 and 4, which also indicated that these two brain regions of sorafenib-treated rats could be clearly separated from control rats. The loadings were colored according to the UV model variable weights and showed the significant class-discriminating metabolites responsible for the clustering patterns. The positive signals indicated the upregulated metabolites in drug-treated group in comparison with the normal controls. Additionally, the signals in the negative direction indicated the downregulated metabolites in drug-treated group.

Metabolic Alterations of Brain Regions in Sorafenib-Treated Rats

We identified that the metabonomics profiles in hippocampus, striatum, and PFC were modified by sorafenib. Interestingly, the metabolites in hippocampus were altered more extensively and significantly among these three

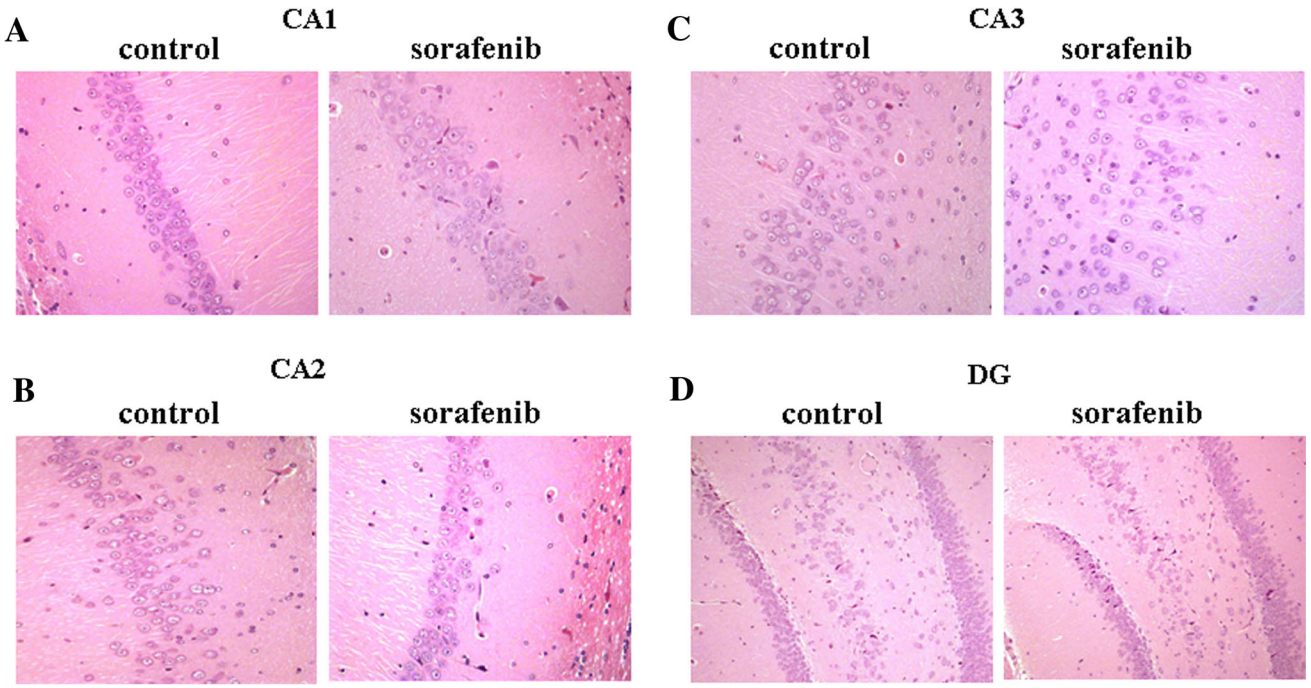

Fig. 1 Histological examination of hippocampus tissue (×400). Hematoxylin and eosin-stained sections of hippocampus CA1 (**a**), CA2 (**b**), CA3 (**c**), DG (**d**) from sorafenib-treated rats and control rats

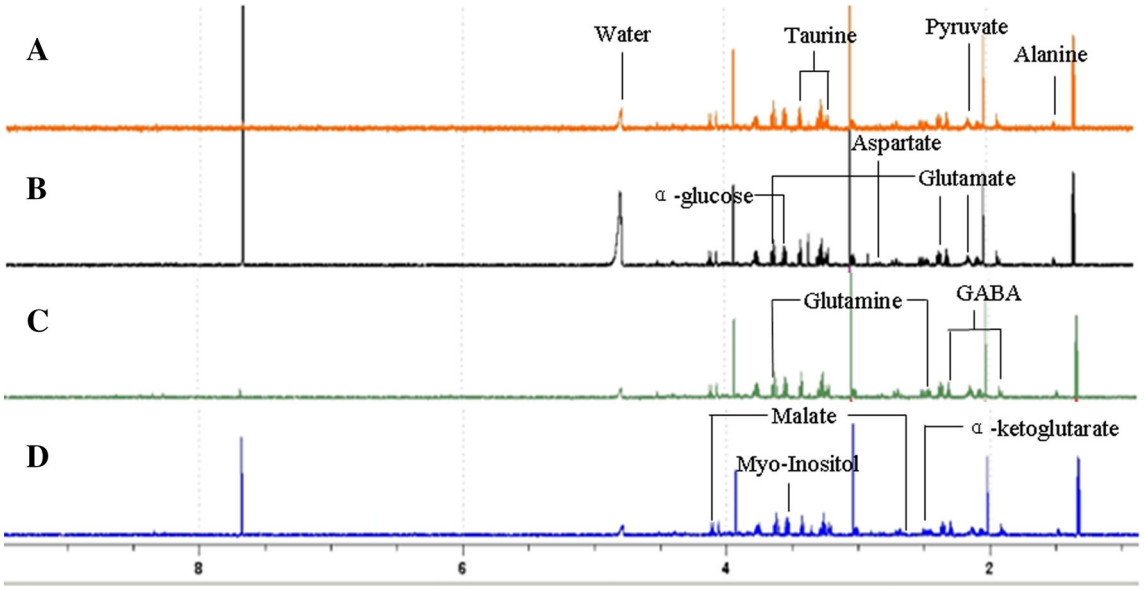

Fig. 2 600 MHz representative 1H NMR spectra (δ 9.5–δ 0.5) of hippocampus from control rats and sorafenib-treated rats: control rats (**a**); sorafenib administration for 3 days (**b**); sorafenib administration for 7 days (**c**); sorafenib administration for 28 days (**d**). The metabolites showing differences in the concentration between sorafenib and control groups are labeled

regions. Our results showed that a panel of 36 metabolites in hippocampus with VIP > 1 from the training set and $p < 0.05$ from Student's t test are identified and summarized in Table 1. These metabolites are involved in the key metabolic pathways, including neurotransmitters, energy metabolism, membrane, and amino acids. However, only a few metabolites in striatum and PFC were modified, as listed in Tables 2 and 3, separately. Since hippocampus plays an important role in learning, memory, and cognitive function, we focused on this region in our study. Then, the representative metabolites with significant difference in hippocampus were represented in box-and-whisker plots (Fig. 4), which showed the concentration ranges, median quartiles, and extremes.

Metabolic Changes in Neurotransmitters

Compared with the vehicle, sorafenib administration led to a significant decrease of the total amount of the detectable neurotransmitters in hippocampus, including GABA, glutamate, and glutamine, of which were reduced markedly along with the progression of sorafenib administration (Table 1; Fig. 4). Moreover, glutamate was also decreased in striatum after sorafenib administration for 28 days (Table 2). But these neurotransmitters showed no abnormalities in PFC (Table 3).

Modifications in Energy Metabolism

Glucose, the main source of energy metabolism and precursors for biosynthesis of macromolecules in cells, was decreased dramatically in hippocampus along with the progression of sorafenib administration (Table 1; Fig. 4); however, glucose was not changed in striatum and PFC (Tables 2, 3). Studies demonstrate that lactate is an alternative energy source in brain (Pellerin 2003; Duarte et al. 2015). Interestingly, our results showed that the level of lactate in hippocampus was declined clearly after sorafenib administration for both 7 and 28 days. However, the declined lactate was only showed in PFC after sorafenib administration for 7 days. No change for lactate was discovered in striatum.

Metabolites related to citric acid cycle, such as malate, pyruvate, and α-ketoglutarate, were significantly modified by sorafenib. Both malate and pyruvate were declined in hippocampus after sorafenib treatment for 28 days (Table 1; Fig. 4). But malate was increased in striatum at day 7 and in PFC at day 28 during the period of sorafenib treatment. In addition, α-ketoglutarate was slightly increased in hippocampus after 7 days' treatment, whereas it was not altered in other two brain regions.

Disruptions of Membrane and Amino Acids

As listed in Table 1, membrane ingredients like phosphatidylcholine in hippocampus and striatum were declined in response to sorafenib; however, they showed no obvious alterations in PFC. Myo-inositol was also decreased by sorafenib in hippocampus (Fig. 4). Furthermore, some amino acids in hippocampus, such as alanine, proline, aspartate, and lysine, were markedly decreased along with the progression of sorafenib administration

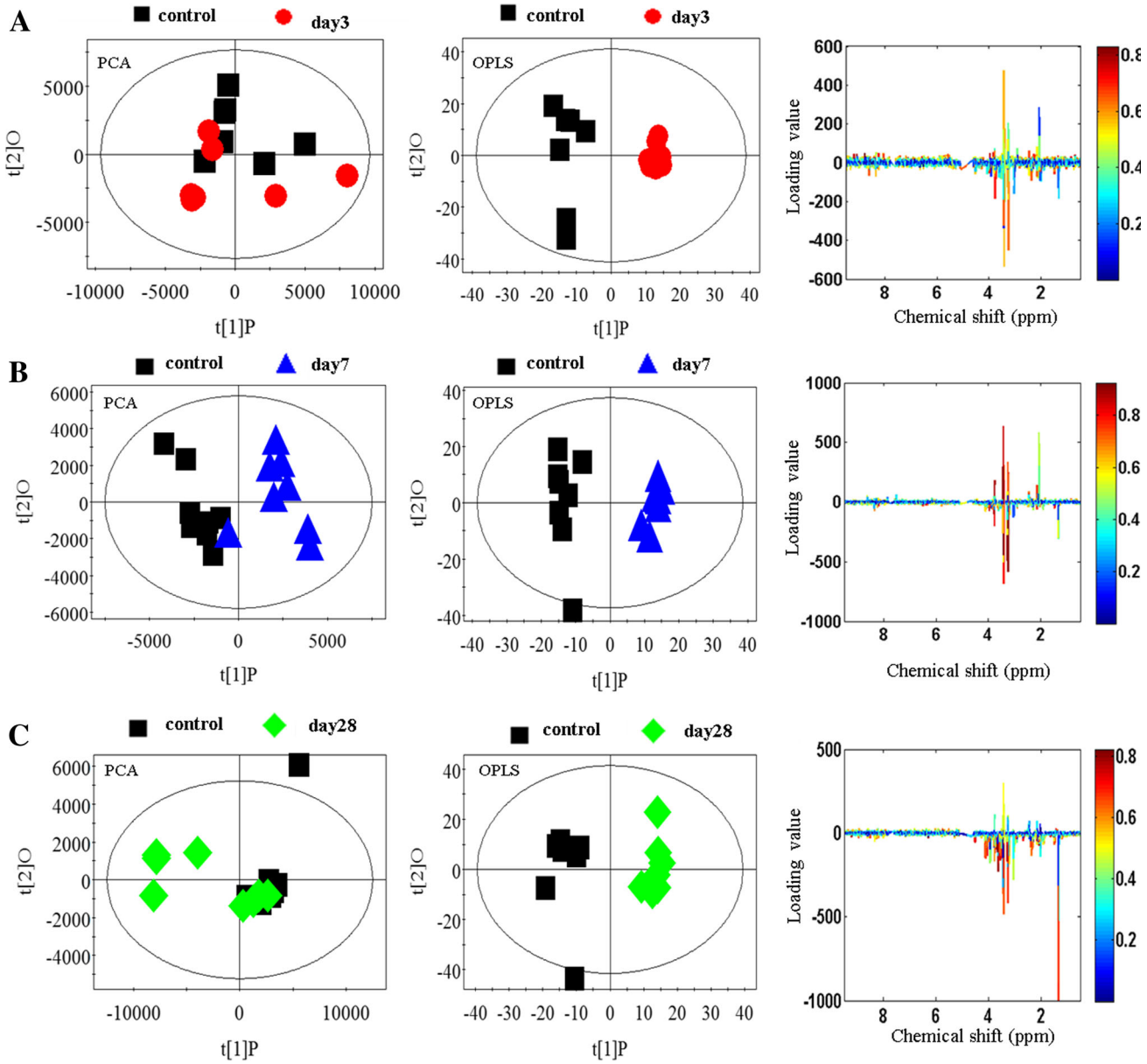

Fig. 3 Metabolite profiles of the hippocampus between different stages of sorafenib-treated rats and the control rats. **a** PCA scores plot, OPLS-DA scores plots, and color map of the rats treated with sorafenib for 3 days ($n = 6$); control rats ($n = 7$); **b** PCA scores plot, OPLS-DA scores plots, and color map of the rats treated with sorafenib for 7 days ($n = 8$); control rats ($n = 7$); **c** PCA scores plot, OPLS-DA scores plots, and color map of the rats treated with sorafenib for 28 days ($n = 7$); control rats ($n = 7$); Color map showed the significance of metabolite variations between the classes. Peaks in the positive direction indicated the increased metabolites in sorafenib-treated rat tissues, while decreased metabolites in sorafenib-treated rats were presented as peaks in the negative direction

(Table 1; Fig. 4). However, these amino acids showed no change in PFC (Table 3). A small elevation in aspartate in striatum was induced after sorafenib treatment for 3 days (Table 2).

Disturbances of Antioxidants and Other Metabolites

Taurine, which possesses the antioxidant property, was significantly declined in hippocampus after sorafenib treatment for both 7 and 28 days (Fig. 4). Taurine also declined in striatum after 28 days' administration of sorafenib. However, it was increased in PFC at 3 days after drug administration. Downregulation of creatine and phosphocreatine in hippocampus along with the progression of drug treatment was observed (Table 1; Fig. 4), while such decrease in striatum and PFC was not observed (Tables 2, 3). Downregulation of TMAO in hippocampus was induced by drug treatment.

Table 1 Summary of the variations from hippocampus metabolites in mice

Metabolites	Chemical shift (ppm)	Multiplicity[a]	Control vs. day 3		Control vs. day 7		Control vs. day 28	
			VIP[a]	FC[b]	VIP[a]	FC[b]	VIP[a]	FC[b]
Isoleucine	0.95	t					2.04	−3.2
Lactate	1.33	d			1.80	−1.14	2.05	−1.5
Lactate	4.11	q			2.16	−1.22	2.07	−1.5
Threonine	1.33	d			1.80	−1.14	2.05	−1.5
Alanine	1.48	d			2.69	−1.15	1.95	−1.3
Alanine	3.76	d					2.50	−1.2
GABA	1.91	s					2.00	−1.3
GABA	2.3	t					1.96	−1.3
Proline	2.35	m					2.22	−1.2
Glutamate	2.1	m					2.51	−1.3
Glutamate	2.35	m					2.22	−1.2
Glutamate	3.77	m					2.50	−1.2
Glutamine	3.77	m					2.50	−1.2
Acetoacetate	2.28	s					1.96	−1.3
Pyruvate	2.37	s					2.22	−1.2
Malate	2.64	m					2.28	−1.4
Malate	4.29	t			2.25	−1.36		
Carnitine	2.44	m			2.79	1.15		
α-ketoglutarate	2.45	t			2.79	1.12		
Glutathione	2.56	m						−1.1
Aspartate	2.82	dd					1.95	−1.2
Methylguanidine	2.81	3					1.60	−1.2
Phosphocreatine	3.04	s					1.20	−1.1
Phosphocreatine	3.93	s					1.09	−1.1
Creatine	3.04	s					1.20	−1.1
Creatine	3.94	s					1.09	−1.1
PC (phosphochline)	3.21	s					1.20	−1.5
Choline	3.2	s					1.66	−1.5
GPC	3.23	s			2.00	−1.24		
Taurine	3.27	t			2.99	−1.11	2.48	−1.2
Taurine	3.43	t			3.01	−1.12	2.14	−1.2
Trimethylamine-*N*-oxide	3.27	s			2.98	−1.16		
TMAO	3.27	s			2.98	−1.16		
Myo-Inositol	3.53	dd					2.35	−1.3
α-glucose	3.55	dd					2.35	−1.3
Glycerol	3.57	s			2.05	−1.09		
Glycerol	3.64	m			2.12	−1.11	2.51	−1.2
Glycerol	3.79	m			2.81	−1.21		
Glycine	3.57	tt			2.05	−1.47		
Lysine	3.77	m					2.50	−1.2
Mannitol	3.77	m					2.50	−1.2
	3.81	m			1.87	−1.13		
Glycolate	3.93	s					1.09	2.12
Serine	3.98	m			2.80	−1.19	2.08	−1.17
Glyceryl	4.3	m			2.25	−1.26		
Tyrosine	7.2	d	2.04	5.1				
NMN	9.31	d	1.37	−3.2				

Table 1 continued

Metabolites	Chemical shift (ppm)	Multiplicity[a]	Control vs. day 3		Control vs. day 7		Control vs. day 28	
			VIP[a]	FC[b]	VIP[a]	FC[b]	VIP[a]	FC[b]
Formate	8.45	s	1.95	8.67	1.60	−1.8		

s Singlet, *d* doublet, *t* triplet, *q* quartet, *dd* doublet of doublets, *m* multiplet

[a] Variable importance in the projection was obtained from OPLS-DA model with a threshold of 1.0

[b] Fold change(FC) between sorafenib-treated rats and controls. Fold change with a positive value indicates a relatively higher concentration present in sorafenib-treated rats, while a negative value means a relatively lower concentration as compared to the normal controls

Table 2 Summary of the variations from striatum metabolites in mice

Metabolites	Chemical shift (ppm)	Multiplicity	Control vs. day 3		Control vs. day 7		Control vs. day 28	
			VIP[a]	FC[b]	VIP[a]	FC[b]	VIP[a]	FC[b]
β-hydroxybutyrate	1.2	d	1.85	5.6				
Glutamate	2.1	m					2.53	−1.3
Malate	4.29	t			1.66	1.38		
Aspartate	2.82	dd	2.11	1.26				
Methylguanidine	2.81	3	1.92	1.16				
PC (phosphochline)	3.21	s					2.15	−1.4
Choline	3.2	s					2.15	−1.4
Taurine	3.43	t					1.71	−1.1

s Singlet, *d* doublet, *t* triplet, *q* quartet, *dd* doublet of doublets, *m* multiplet

[a] Variable importance in the projection was obtained from OPLS-DA model with a threshold of 1.0

[b] Fold change(FC) between sorafenib-treated rats and controls. Fold change with a positive value indicates a relatively higher concentration present in sorafenib-treated rats, while a negative value means a relatively lower concentration as compared to the normal controls

Table 3 Summary of the variations from PFC metabolites in mice

Metabolites	Chemical shift (ppm)	Multiplicity	Control vs. day 3		Control vs. day 7		Control vs. day 28	
			VIP[a]	FC[b]	VIP[a]	FC[b]	VIP[a]	FC[b]
Lactate	4.11	q			2.14	−4.09		
Malate	2.64	m					1.886	2.4
Glutathione	2.96	m	2.2	1.14				
Taurine	3.43	t	1.9	2.86				
Glycine	3.57	tt					1.659	1.64
Glyceryl	4.17	m					2.574	3.05
NMN	9.31	d			2.45	−2.04		
Formate	8.45	s			1.93	−4.18		

s Singlet, *d* doublet, *t* triplet, *q* quartet, *dd* doublet of doublets, *m* multiplet

[a] Variable importance in the projection was obtained from OPLS-DA model with a threshold of 1.0

[b] Fold change(FC) between sorafenib-treated rats and controls. Fold change with a positive value indicates a relatively higher concentration present in sorafenib-treated rats, while a negative value means a relatively lower concentration as compared to the normal controls

Discussion

The negative cognitive functioning has been observed in cancer patients with VEGF inhibitor treatment for many years, but mechanisms for such clinical adverse effect remain blank (Vardy and Tannock 2007; Ahles and Saykin 2007; Takimoto and Awada 2008). Because hippocampus, striatum, and PFC play important roles in memory and cognitive function (Addante 2015; Shu et al. 2014; Keller et al. 2015), we thus chose these three brain regions for this

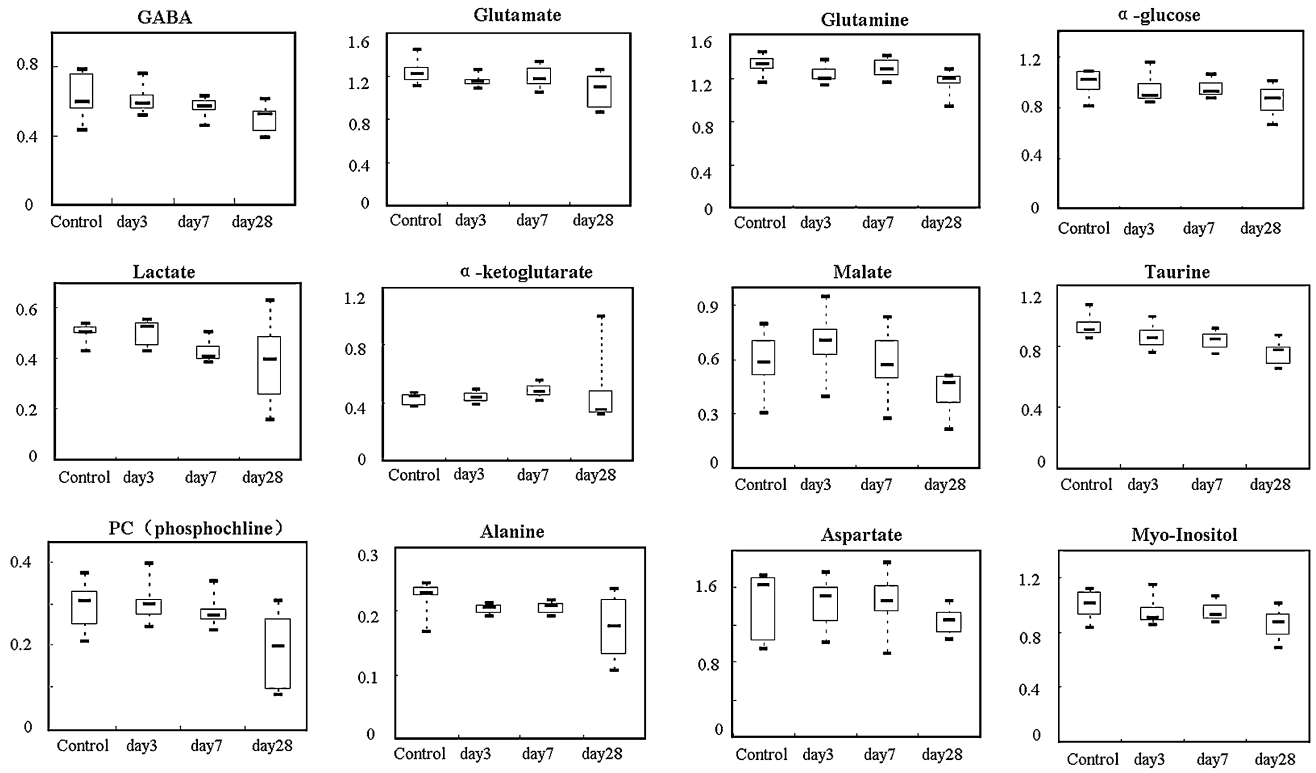

Fig. 4 Fold of changes in levels of identified metabolites from ^{1}H NMR spectra in sorafenib-treated rats and control rats in the hippocampus. This figure shows the time-dependent biochemical variations induced by sorafenib

study. As metabonomics provide a promising opportunity to generate novel biomarkers and hypothesis for addressing the molecular mechanisms of diseases (Ni et al. 2008), we analyzed the metabolic profiles of hippocampus, striatum, and PFC from sorafenib-treated rats. Here, we found that sorafenib caused significant disturbances in the endogenous metabolite profiles, especially, in hippocampus that is associated with learning and memory. The disturbed biochemical metabolisms and pathways involved in neurotransmitters, energy metabolism, membrane, and free amino acids. However, metabonomics alterations in striatum and PFC were not obvious. Our findings reveal the disturbed metabonomics profile in hippocampus, which may underlie the sorafenib-induced neurotoxicological effects in patients.

In the present study, the general behavioral symptoms were not noted in sorafenib-treated rats. Also, histopathology examination for brain showed no abnormality. However, NMR-PR analyses of brain highlighted some complex disturbances in endogenous metabolites profiles, which could be closely related to the sorafenib-modified biochemical pathways. Therefore, ^{1}H NMR technique-based metabolomics provides a sensitive methodology and a systematic insight for investigating the biochemical effect of drugs and underlying mechanism.

Disturbance in Neurotransmitters

We found that the concentrations of GABA, glutamine, and glutamate were remarkably decreased in hippocampus of sorafenib-treated rats; glutamate was also declined in striatum. The potential reason for such repression of glutamatergic transmission could be the decreased de novo synthesis via citric acid cycle. Since α-ketoglutarate can be transferred into glutamate via glutamate syntheses (Brown and Yamamoto 2003; Bu et al. 2013), the decreased α-ketoglutarate in this study may contribute to the down-regulated glutamine synthesis.

GABA, a key mediator of inhibitory neurotransmission in mammalian central nervous system, is generated from glutamate in GABAergic neurons by glutamic acid decarboxylase (GAD) (Sa Santos et al. 2011). The decreased glutamate may directly lead to a lower GABA production. It is reported that glutaminase activity is pivotal for the synthesis of GABA from glutamine (Holten and Gundersen 2008). We guess that decreased GAD activity in

hippocampus of sorafenib-treated rats may attribute to the declined GABA production.

Dysregulation in Energy Metabolism

Studies have showed that memory formation increases synaptic transmission and morphological alterations at the synapse, both of which consume more energy in the neuron (Bontempi et al. 1999; Thiagarajan et al. 2005). Metabolites of glucose, lactate, malate, and α-ketoglutarate were remarkably decreased in hippocampus of sorafenib-treated rats, and the decline of lactate also occurred in PFC. Because glucose and lactate are the first and the end-product of glycolysis, respectively, the declines of these two metabolites indicated the inhibition of glycolysis as well as insufficient energy substrate (Wang et al. 2013a). Lactate has been shown to play roles in adult central nervous system, such as sustaining electrical activity of hippocampus and protecting neurons against NMDA-induced neurotoxicity (Pellerin 2003). Therefore, the decreased lactate may weaken the normal electrical activity of hippocampus.

Citrate and α-ketoglutarate are dominant products of citric acid cycle, and the decreased levels of these two metabolites in this study were associated with weakened glycometabolism and energy metabolism. These results are in consistent with the aforementioned observation of inhibited glycolysis. Collectively, dysregulation of energy metabolism caused by sorafenib implicates a repressed energetic metabolism in the brain, suggesting the lower neuron activity and neuroplasticity especially in the hippocampus.

Disruption of Membrane

Phospholipids are essential components of cell membranes. Phosphocholine and myo-inositol are precursors used for synthesis of membrane phospholipids in the cell and their

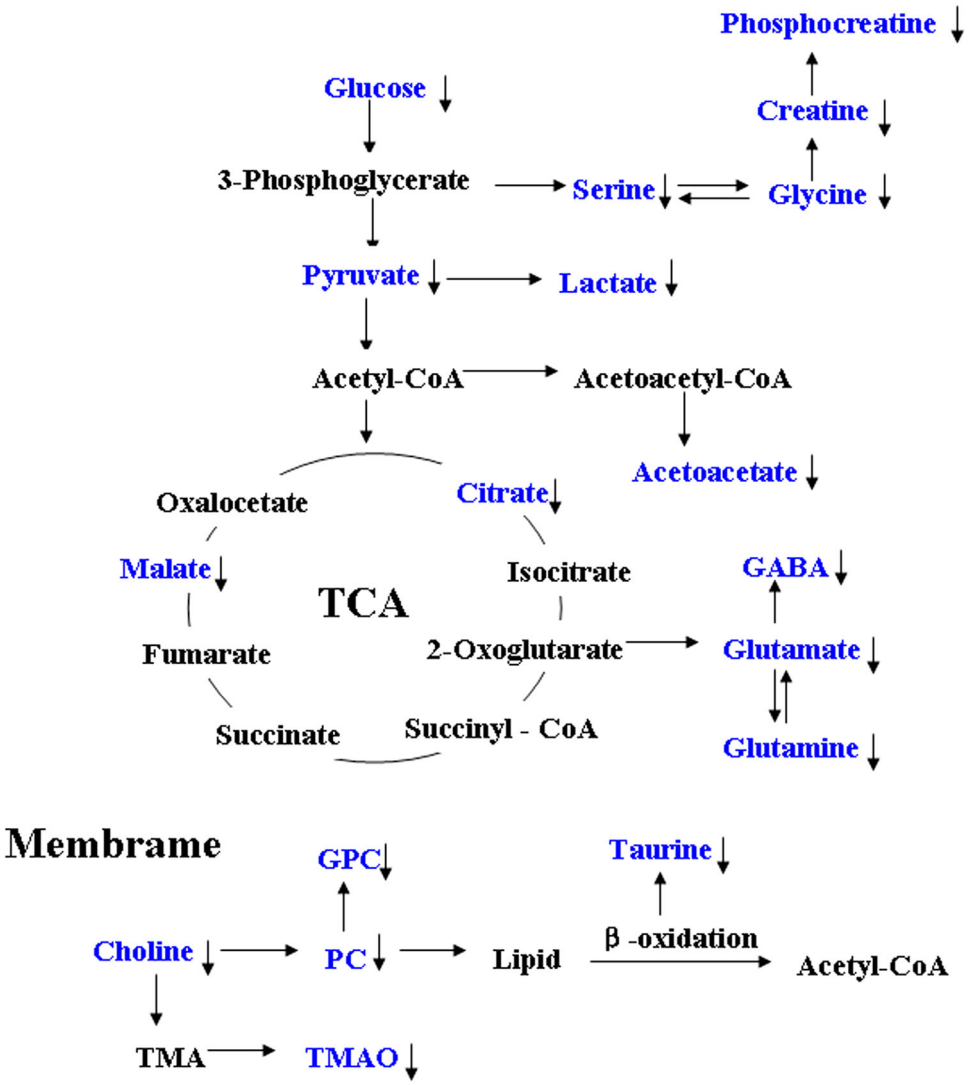

Fig. 5 Disturbed metabolic pathways of the most relevant metabolites between sorafenib-treated rats and control rats. "↓" represents the decreased metabolites in sorafenib-treated rats

levels play a role in lipid metabolism (Lan et al. 2009). Phosphocholine contributes to the choline resonance, which may act as a biomarker for membrane phospholipid metabolism (Senaratne et al. 2009). Moreover, myo-inositol is a significant intracellular osmolyte, whose change may indicate alterations in tissue osmolarity (Lan et al. 2009). Therefore, decreases in phosphocholine and myo-inositol in hippocampus of the sorafenib-treated rats may be the potential indication of cell membrane disruption or deceased membrane turnover.

Disturbances of Antioxidants and Other Metabolites

Taurine has been suggested to be a neuroprotective chemical (Zhou et al. 2011), and its effects include calcium modulation, apoptosis inhibition, and antioxidant properties (Wu et al. 2005; Oja and Saransaari 2007). Creatine is thought to exert direct antioxidant effects and to normalize mitochondrial mutagenesis (Guidi et al. 2008). In the present study, both taurine and creatine decreased obviously in hippocampus of sorafenib-treated rats. Such decreases may reflect the exhaustion of antioxidant and a weakened protective capability.

It has been known that disorder of amino acid metabolism can be induced by proteolysis, oxidative catabolism, and gluconeogenesis (Li et al. 2014). In pathological status, amino acids as substrates are highly demanded for energy production, such as infection and cancer (Sreekumar et al. 2009). In our study, the levels of alanine, proline, aspartate, and lysine in hippocampus were significantly downregulated by sorafenib. These results are supported by the aforementioned findings that sorafenib decreased hippocampal glucose and energy metabolism. Because these amino acids belong to essential amino acids, non-essential amino acids, or amino acid with putative neurotransmitter function, sorafenib may extensively influence protein metabolism as well neurotransmitter through modifying amino acids in brain.

In our study, metabolites in hippocampus of sorafenib-treated rats decreased significantly as compared with PFC and striatum. Based on these modified metabolites, we summarized related metabolic pathways in Fig. 5. The disturbed metabolism and metabolic pathways include neurotransmitters, energy, amino acids, membrane, as well as antioxidants. Generally, sorafenib extensively represses hippocampal energy metabolism, glutamatergic transmission, and antioxidative capacity. As sorafenib selectively targets VEGFR which can affect cerebral blood flow and vascular neogenesis (Schänzer et al. 2004; Ongali et al. 2010; Fournier et al. 2013), we assume that sorafenib may repress brain metabolic activity through affecting blood flow and nutrient supply for brain. Our findings provide not only a new insight into the mechanism, but also a potential therapeutic strategy for sorafenib-related cognitive impairments in patients.

Acknowledgments This work was supported by the National Science & Technology Major Project (2012ZX09302-004) and National Natural Sciences Foundation of China (81271467, 81272459, 30970938).

Compliance with Ethical Standards

Conflict of interest The authors declare that there are no conflicts of interest.

References

Addante RJ (2015) A critical role of the human hippocampus in an electrophysiological measure of implicit memory. Neuroimage 109:515–528

Ahles TA, Saykin AJ (2007) Candidate mechanisms for chemotherapy-induced cognitive changes. Nat Rev Cancer 7:192–201

Beckonert O, Keun HC, Ebbels TM, Bundy J, Holmes E, Lindon JC, Nicholson JK (2007) Metabolic profiling, metabolomic and metabonomic procedures for NMR spectroscopy of urine, plasma, serum and tissue extracts. Nat Protoc 2:2692–2703

Bontempi B, Laurent-Demir C, Destrade C, Jaffard R (1999) Time-dependent reorganization of brain circuitry underlying long-term memory storage. Nature 400:671–675

Brandi G, Rosa F, Calzà L, Girolamo SD, Tufoni M, Ricci CS, Cirignotta F, Caraceni P, Biasco G (2013) Can the tyrosine kinase inhibitors trigger metabolic encephalopathy in cirrhotic patients? Liver Int 33:488–493

Brown JM, Yamamoto BK (2003) Effects of amphetamines on mitochondrial function: role of free radicals and oxidative stress. Pharmacol Ther 99:45–53

Bu Q, Lv L, Yan G, Deng P, Wang Y, Zhou J, Yang Y, Li Y, Cen X (2013) NMR-based metabonomic in hippocampus, nucleus accumbens and prefrontal cortex of methamphetamine-sensitized rats. NeuroToxicology 36:17–23

Dietrich J, Monje M, Wefel J, Meyers C (2008) Clinical patterns and biological correlates of cognitive dysfunction associated with cancer therapy. Oncologist 13:1285–1295

Duarte IF, Ladeirinha AF, Lamego I, Gil AM, Carvalho L, Carreira IM, Melo JB (2013) Potential markers of cisplatin treatment response unveiled by NMR metabolomics of human lung cells. Mol Pharm 10:4242–4251

Duarte JM, Girault FM, Gruetter RJ (2015) Brain energy metabolism measured by (13) C magnetic resonance spectroscopy in vivo upon infusion of [3-(13) C]lactate. J Neurosci Res 93:1009–1018

Fournier NM, Lee B, Banasr M, Elsayed M, Duman RS (2013) Vascular endothelial growth factor regulates adult hippocampal cell proliferation through MEK/ERK- and PI3 K/Akt-dependent signaling. Neuropharmacology 63:642–652

Gao H, Xiang Y, Sun N, Zhu H, Wang Y, Liu M, Ma Y, Lei H (2007) Metabolic changes in rat prefrontal cortex and hippocampus

induced by chronic morphine treatment studied ex vivo by high resolution 1H NMR spectroscopy. Neurochem Int 50:386–394
Guidi C, Potenza L, Sestili P, Martinelli C, Guescini M, Stocchi L, Zeppa S, Polidori E, Annibalini G, Stocchi V (2008) Differential effect of creatine on oxidatively-injured mitochondrial and nuclear DNA. Biochim Biophys Acta 1780:16–26
Holten AT, Gundersen V (2008) Glutamine as a precursor for transmitter glutamate, aspartate and GABA in the cerebellum: a role for phosphate-activated glutaminase. J Neurochem 104: 1032–1042
Hu Z, Deng Y, Hu C, Deng P, Bu Q, Yan G, Zhou J, Shao X, Zhao J, Li Y (2012) 1 H NMR-based metabonomic analysis of brain in rats of morphine dependence and withdrawal intervention. Behav Brain Res 231:11–19
Jung JY, Lee HS, Kang DG, Kim NS, Cha MH, Bang OS, Ryu do H, Hwang GS (2011) 1H-NMR-based metabolomics study of cerebral infarction. Stroke 42:1282–1288
Kaddurah-Daouk R, Krishnan KR (2009) Metabolomics: a global biochemical approach to the study of central nervous system diseases. Neuropsychopharmacology 34:173–186
Kaddurah-Daouk R, Kristal BS, Weinshilboum RM (2008) Metabolomics: a global biochemical approach to drug response and disease. Annu Rev Pharmacol Toxicol 48:653–683
Kane RC, Farrell AT, Saber H, Tang S, Williams G, Jee JM, Liang C, Booth B, Chidambaram N, Morse D, Sridhara R, Garvey P, Justice R, Pazdur R (2006) Sorafenib for the treatment of advanced renal cell carcinoma. Clin Cancer Res 12:7271–7278
Keller JB, Hedden T, Thompson TW, Anteraper SA, Gabrieli JD, Whitfield-Gabrieli S (2015) Resting-state anticorrelations between medial and lateral prefrontal cortex: association with working memory, aging, and individual differences. Cortex 64:271–280
Krishnan P, Kruger N, Ratcliffe R (2005) Metabolite fingerprinting and profiling in plants using NMR. J Exp Bot 56:255–265
Kuroi K, Shimozuma K (2004) Neurotoxicity of taxanes: symptoms and quality of life assessment. Breast Cancer 11:92–99
Lan MJ, McLoughlin GA, Griffin JL, Tsang TM, Huang JT, Yuan P, Manji H, Holmes E, Bahn S (2009) Metabonomic analysis identifies molecular changes associated with the pathophysiology and drug treatment of bipolar disorder. Mol Psychiatry 14:269–279
Li H, Bu Q, Chen B, Shao X, Hu Z, Deng P, Lv L, Deng Y, Zhu R, Li Y, Zhang B, Hou J, Du C, Zhao Q, Fu D, Zhao Y, Cen X (2014) Mechanisms of metabonomic for a gateway drug: nicotine priming enhances behavioral response to cocaine with modification in energy metabolism and neurotransmitter level. PLoS One 9:e87040
McClay JL, Adkins DE, Vunck SA, Batman AM, Vann RE, Clark SL, Beardsley PM, van den Oord EJ (2013) Large-scale neurochemical metabolomics analysis identifies multiple compounds associated with methamphetamine exposure. Metabolomics 9: 392–402
Mulder SF, Bertens D, Desar IM, Vissers KC, Mulders PF, Punt CJ, van Spronsen DJ, Langenhuijsen JF, Kessels RP, van Herpen CM (2014) Impairment of cognitive functioning during Sunitinib or Sorafenib treatment in cancer patients: a cross sectional study. BMC Cancer 14:219
Ni Y, Su M, Lin J, Wang X, Qiu Y, Zhao A, Chen T, Jia W (2008) Metabolic profiling reveals disorder of amino acid metabolism in four brain regions from a rat model of chronic unpredictable mild stress. FEBS Lett 582:2627–2636
Oja SS, Saransaari P (2007) Pharmacology of taurine. Proc West Pharmacol Soc 50:8–15
Ongali B, Nicolakakis N, Lecrux C, Aboulkassim T, Rosa-Neto P, Papadopoulos P, Tong X-K, Hamel Edith (2010) Transgenic mice overexpressing APP and transforming growth factor-β1 feature cognitive and vascular hallmarks of Alzheimer's disease. Am J Pathol 177:3071–3080
Pellerin L (2003) Lactate as a pivotal element in neuron–glia metabolic cooperation. Neurochem Int 43:331–338
Sa Santos S, Sonnewald U, Carrondo MJ, Alves PM (2011) The role of glia in neuronal recovery following anoxia: in vitro evidence of neuronal adaptation. Neurochem Int 58:665–675
Salek RM, Colebrooke RE, Macintosh R, Lynch PJ, Sweatman BC, Emson PC, Griffin JL (2008) A metabolomic study of brain tissues from aged mice with low expression of the vesicular monoamine transporter 2 (VMAT2) gene. Neurochem Res 33:292–300
Schänzer A, Wachs FP, Wilhelm D, Acker T, Cooper-Kuhn C, Beck H, Winkler J, Aigner L, Plate KH, Kuhn HG (2004) Direct stimulation of adult neural stem cells in vitro and neurogenesis in vivo by vascular endothelial growth factor. Brain Pathol 14:237–248
Senaratne R, Milne AM, MacQueen GM, Hall GB (2009) Increased choline-containing compounds in the orbitofrontal cortex and hippocampus in euthymic patients with bipolar disorder: a proton magnetic resonance spectroscopy study. Psychiatry Res 172:205–209
Shu S-Y, Jiang G, Zeng Q-Y, Wang B, Li H, Ma L, Steinbusch H, Song C, Chan W-Y, Chen X-H (2014) The marginal division of the striatum and hippocampus has different role and mechanism in learning and memory. Mol Neurobiol 51:827–839
Sreekumar A, Poisson LM, Rajendiran TM, Khan AP, Cao Q, Yu J, Laxman B, Mehra R, Lonigro RJ, Li Y, Nyati MK, Ahsan A, Kalyana-Sundaram S, Han B, Cao X, Byun J, Omenn GS, Ghosh D, Pennathur S, Alexander DC, Berger A, Shuster JR, Wei JT, Varambally S, Beecher C, Chinnaiyan AM (2009) Metabolomic profiles delineate potential role for sarcosine in prostate cancer progression. Nature 457:910–914
Takimoto CH, Awada A (2008) Safety and anti-tumor activity of sorafenib (Nexavar) in combination with other anti-cancer agents: a review of clinical trials. Cancer Chemother Pharmacol 61:535–548
Thiagarajan TC, Lindskog M, Tsien RW (2005) Adaptation to synaptic inactivity in hippocampal neurons. Neuron 47:725–737
Vardy J, Tannock I (2007) Cognitive function after chemotherapy in adults with solid tumours. Crit Rev Oncol Hematol 63:183–202
Wang H, Wang L, Zhang H, Deng P, Chen J, Zhou B, Hu J, Zou J, Lu W, Xiang P (2013a) H NMR-based metabolic profiling of human rectal cancer tissue. Mol Cancer 12:121
Wang L, Chen J, Chen L, Deng P, Bu Q, Xiang P, Li M, Lu W, Xu Y (2013b) 1H-NMR based metabonomic profiling of human esophageal cancer tissue. Mol Cancer 12:25
Wishart DS, Tzur D, Knox C, Eisner R, Guo AC, Young N, Cheng D, Jewell K, Arndt D, Sawhney S, Fung C, Nikolai L, Lewis M, Coutouly MA, Forsythe I, Tang P, Shrivastava S, Jeroncic K, Stothard P, Amegbey G, Block D, Hau DD, Wagner J, Miniaci J, Clements M, Gebremedhin M, Guo N, Zhang Y, Duggan GE, Macinnis GD, Weljie AM, Dowlatabadi R, Bamforth F, Clive D, Greiner R, Li L, Marrie T, Sykes BD, Vogel HJ, Querengesser L (2007) HMDB: the human metabolome database. Nucleic Acids Res 35:D521–D526
Wu H, Jin Y, Wei J, Jin H, Sha D, Wu J-Y (2005) Mode of action of taurine as a neuroprotector. Brain Res 1038:123–131
Xiang Y, Gao H, Zhu H, Sun N, Ma Y, Lei H (2006) Neurochemical changes in brain induced by chronic morphine treatment: NMR studies in thalamus and somatosensory cortex of rats. Neurochem Res 31:1255–1261
Zhou J, Li Y, Yan G, Bu Q, Lv L, Yang Y, Zhao J, Shao X, Deng Y, Zhu R (2011) Protective role of taurine against morphine-induced neurotoxicity in C6 cells via inhibition of oxidative stress. Neurotox Res 20:334–342